

RIS-Aided Multiuser MIMO-OFDM with Linear Precoding and Iterative Detection: Analysis and Optimization

Mingyang Yue, Lei Liu, *Member, IEEE*, and Xiaojun Yuan, *Senior Member, IEEE*

Abstract

In this paper, we consider a reconfigurable intelligence surface (RIS) aided uplink multiuser multi-input multi-output (MIMO) orthogonal frequency division multiplexing (OFDM) system, where the receiver is assumed to conduct low-complexity iterative detection. We aim to minimize the total transmit power by jointly designing the precoder of the transmitter and the passive beamforming of the RIS. This problem can be tackled from the perspective of information theory. But this information-theoretic approach may involve prohibitively high complexity since the number of rate constraints that specify the capacity region of the uplink multiuser channel is exponential in the number of users. To avoid this difficulty, we formulate the design problem of the iterative receiver under the constraints of a maximal iteration number and target bit error rates of users. To tackle this challenging problem, we propose a groupwise successive interference cancellation (SIC) optimization approach, where the signals of users are decoded and cancelled in a group-by-group manner. We present a heuristic user grouping strategy, and resort to the alternating optimization technique to iteratively solve the precoding and passive beamforming sub-problems. Specifically, for the precoding sub-problem, we employ fractional programming to convert it to a convex problem; for the passive beamforming sub-problem, we adopt successive convex approximation to deal with the unit-modulus constraints of the RIS. We show that the proposed groupwise SIC approach has significant advantages in both performance and computational complexity, as compared with the counterpart approaches.

Mingyang Yue and Xiaojun Yuan are with the National Key Laboratory of Science and Technology on Communications, University of Electronic Science and Technology of China, Chengdu 611731, China (e-mail: myyue@std.uestc.edu.cn; xjyuan@uestc.edu.cn).

Lei Liu is with the School of Information Science, Japan Advanced Institute of Science and Technology, Nomi 923-1292, Japan (e-mail: leiliu@jaist.ac.jp).

Index Terms

Reconfigure intelligent surface, MIMO-OFDM, precoding, passive beamforming, iterative detection

I. INTRODUCTION

Reconfigurable intelligent surface (RIS) has been regarded as a key enabling technology for the sixth-generation (6G) wireless communications [1]. RIS is composed of a large number of low-cost passive reflecting elements, where a controller is equipped to adjust the reflection coefficient of each element in real time. By effectively designing the passive beamforming of the elements, RIS can reconfigure the wireless propagation environment by intelligently manipulating the reflection direction of the incident electromagnetic wave. In addition, RIS also has the advantages of flexible deployment, low energy consumption, and low noise [2]. Extensive research has been conducted on the design of RIS to improve the system performance in terms of energy and spectral efficiency [3]–[7] and channel capacity [8]–[10].

The optimization of RIS to improve the performance of multiuser systems has been investigated, e.g., in [3], [5], [11]–[18]. Particularly, the authors in [11] considered a RIS-aided downlink multiuser system, and designed the active and passive beamforming to maximize the minimal user rate. Ref. [12] aimed to minimize the total transmit power under the user rate constraints for the RIS-aided downlink multiuser multiple-input-single-output (MISO) system. Ref. [13] proposed a difference-of-convex algorithm to jointly design active and passive beamforming by minimizing the total transmit power of all users. The (weighted) sum rate of the multiuser system has been studied in [14] and [15], and has been extended to other scenarios, such as millimeter wave [16], [17] and multi-RIS-aided cooperative transmission [18]. Furthermore, the energy efficiency, defined as the sum rate normalized by the energy consumption, is investigated for RIS aided downlink systems [4] and multiple-input-multiple-output (MIMO) uplink systems [3], [5].

The above works are designed from the perspective of information-theoretic performance metrics. In other words, these works assumed an ideal receiver that can achieve the capacity of the system. However, it is so-far unclear how to design a practical low-complexity receiver to achieve the capacity of the RIS-aided multiuser MIMO channel. In fact, a practical low-complexity receiver may perform quite far away from the capacity, and the capacity-based optimizations may not achieve the expected performance in a practical system with limited computational

capability. Therefore, it is desirable to optimize the performance of the RIS-aided system based on more practical performance metrics rather than on information-theoretic metrics.

In this paper, we study the design of the RIS-aided uplink multiuser MIMO orthogonal frequency division multiplexing (OFDM) system equipped with a practical low-complexity transceiver. Specifically, we adopt the low-complexity receiver with iterative linear minimum-mean-square-error (LMMSE) detection and decoding, which has been previously studied in traditional communication systems [19]–[22]. In [19], the authors proposed the low-complexity iterative detection framework, and established a signal-to-interference-plus-noise ratio (SINR) variance state evolution technique to characterize the performance. Ref. [20] studied the linear precoder design for the iterative receiver. In [21], the authors discussed the achievable rate in a single-user system based on the iterative receiver, and showed that the water-filling channel capacity can be achieved by appropriate precoder design. Furthermore, [22] showed that for the MIMO-NOMA system this receiver can achieve the sum capacity with appropriately designed channel codes.

We aim to jointly design the precoder of transmitter and the passive beamforming of RIS, to minimize the total transmit power for the uplink multiuser MIMO-OFDM system. This optimization problem can be solved by extending the approach in [23] to the multiuser scenario. Yet, the number of rate constraints that specifies the capacity region of the multiuser access channel (MAC) channel is exponential in the number of users. Thus, this information-theoretic approach will cause a prohibitively high complexity in practice, even for a MAC channel with a moderate number of users.

To address this issue, we formulate the joint optimization problem for the iterative LMMSE receiver under the constraints of maximal iteration number and allowed bit error rate (BER). The path condition for BER constraint is derived via the state evolution (SE) [19], where a feasible path needs to be found in a high-dimension variance space. This optimization is challenging even for a traditional multiuser MIMO-OFDM systems without RIS [24], let alone the handling of the extra non-convex constraints of the RIS phase adjustments. To tackle this problem, we propose a group successive interference cancellation (SIC) approach, where users are decoded and cancelled in a group-by-group manner. We first fix the user grouping, and resort to the alternating optimization for precoding and passive beamforming. Specifically, we convert the precoding subproblem to a convex problem by using the fractional programming method [25]. For the subproblem of passive beamforming, we adopt the successive convex approximation to deal with the unit-modulus constraints of RIS. Besides, we propose a heuristic low-complexity user grouping

strategy to avoid the exhaustive search over all possible user groupings. Numerical results show that the proposed groupwise SIC approach substantially outperforms the counterparts, especially when the allowed iteration number of the receiver is relatively small. The contributions of this work are summarised as follows:

- We investigate the joint precoding and passive beamforming design to minimize the total transmit power of the RIS-aided uplink multiuser MIMO-OFDM system. In contrast to the existing works, we consider the system optimization for the low-complexity iterative LMMSE receiver. We establish the state evolution to characterize the system performance, and formulate the joint optimization problem for the iterative receiver under the constraints of target BERs and a maximal iteration number .
- We propose a groupwise SIC approach to solve the challenging optimization problem. We employ a heuristic but efficient user grouping strategy to avoid the exhaustive search over all possible user groupings. For a fixed user grouping, we tackle the problem by alternately solving the precoding and passive beamforming sub-problems. We employ the fractional programming method to convert the precoding sub-problem to a convex problem. We further show that the passive beamforming sub-problem is a feasibility-check problem, which can be solved by skilfully expanding the feasible region and applying successive convex approximation.
- We show that the complexity of the groupwise SIC approach is much lower than that of information-theoretic approach. We also show the groupwise SIC approach substantially outperforms the information-theoretic approach and other counterparts, especially for a relatively small allowed iteration number of the receiver.

The rest of this paper is organized as follows. Section II presents the channel model and the transceiver for a RIS-aided uplink MIMO-NOMA system. In Section III, the state evolution is described, and the optimization problem for the iterative receiver is formulated. In Section IV the groupwise SIC approach is described. Numerical results are provided in Section V. Section VI concludes the paper.

Notions: We use a bold symbol lowercase letter and bold symbol capital letter to denote a vector and a matrix, respectively. The Frobenius norm, trace, transpose, conjugate transpose, and inverse of a matrix are denoted by $\|\cdot\|_F$, $\text{tr}(\cdot)$, $(\cdot)^T$, $(\cdot)^H$ and $(\cdot)^{-1}$, respectively; $[\mathbf{A}]^2$ denotes $\mathbf{A}\mathbf{A}^H$; $\text{diag}(\mathbf{a})$ forms a diagonal matrix with the diagonal elements in \mathbf{a} ; $\|\cdot\|_2$ denotes ℓ_2 -norm

of a vector; $|\cdot|$ denotes the modulus of a complex number; the complex conjugate of a vector is denoted by $(\cdot)^*$; \otimes denotes the Kronecker product; \odot denotes the Hadamard product; $*$ denotes the circular convolution; ∇ denotes the gradient operator; \mathcal{O} is the big-O notation. The complex Gaussian distribution of \mathbf{x} with mean \mathbf{m} and covariance matrix $\mathbf{\Sigma}$ is denoted by $\mathbf{x} \sim \mathcal{CN}(\mathbf{m}, \mathbf{\Sigma})$.

II. SYSTEM MODEL

A. Channel Model

As shown in Fig. 1, we consider an uplink RIS-aided multiuser MIMO-OFDM system, where a RIS with N reflecting elements is deployed to enhance the communication between K single-antenna users and an M -antenna base station (BS). Let J denote the number of subcarriers of each OFDM symbol, and these J subcarriers are shared by all the users. We assume frequency-selective fading channels, and the user-BS, user-RIS and RIS-BS links contain L_{ub} , L_{ur} and L_{rb} taps in the impulse response, respectively [26]. Each user adopts a cyclic prefix (CP) of length L_{cp} with $L_{\text{cp}} \geq \max\{L_{\text{ub}}, L_{\text{ur}} + L_{\text{rb}}\}$ to eliminate inter-symbol interference. Then, the received baseband signal in the time domain at the m th antenna after CP removal is given by

$$\mathbf{r}_m = \sum_{k=1}^K \left(\mathbf{h}_{k,m}^{\text{ub}} + \sum_{n=1}^N \theta_n \mathbf{h}_{k,m,n}^{\text{rb}} * \mathbf{h}_{k,n}^{\text{ur}} \right) * \mathbf{s}_k + \mathbf{n}_m, \quad (1)$$

where $\mathbf{s}_k \in \mathbb{C}^{J \times 1}$ is the transmit signal vector in the time domain, θ_n the reflecting coefficients of the n th RIS element, $\mathbf{h}_{k,m}^{\text{ub}} \in \mathbb{C}^{J \times 1}$ the channel from user k to the BS's m th antenna, $\mathbf{h}_{k,n}^{\text{ur}} \in \mathbb{C}^{J \times 1}$

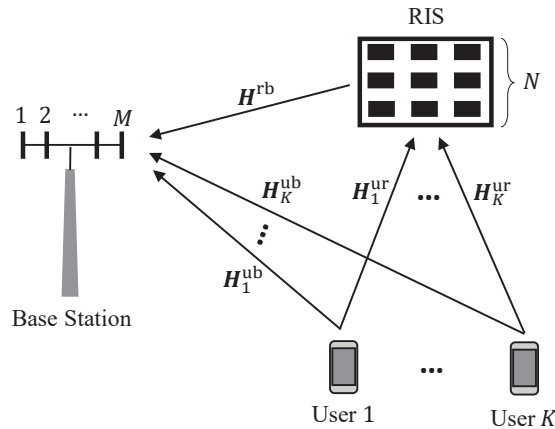


Fig. 1. An uplink multiuser MIMO-OFDM system consisting of K single-antenna users and an M -antenna base station, where a RIS with N elements is deployed to enhance the communication. The channels from user k to the RIS, from user k to the base station and from the RIS to the base station are denoted by \mathbf{H}_k^{ur} , \mathbf{H}_k^{ub} and \mathbf{H}^{rb} , respectively.

the channel from user k to the n th RIS element, $\mathbf{h}_{m,n}^{\text{rb}} \in \mathbb{C}^{J \times 1}$ the channel from the n th RIS element to the BS's m th antenna, and \mathbf{n}_m the additive white Gaussian noise (AWGN). For simplicity, we assume that each θ_n is constant within the considered frequency band. Besides, the phase can be adjusted independently in $[0, 2\pi]$, and all the reflecting coefficients are unit-modulus, i.e., $|\theta_n| = 1, \forall n$. We also assume that perfect channel state information (CSI) is available. In practice, the CSI can be acquired by existing channel estimation methods; see, e.g., [27] and [28].

With (1), the time-domain channel matrix of the direct link between user k and the BS is a block-circulant matrix given by

$$\mathbf{H}_k^{\text{ub}} \triangleq \begin{bmatrix} \mathbf{H}_k^{\text{ub}}(1) & \mathbf{H}_k^{\text{ub}}(J) & \cdots & \mathbf{H}_k^{\text{ub}}(2) \\ \mathbf{H}_k^{\text{ub}}(2) & \mathbf{H}_k^{\text{ub}}(1) & \cdots & \mathbf{H}_k^{\text{ub}}(3) \\ \vdots & \vdots & \ddots & \vdots \\ \mathbf{H}_k^{\text{ub}}(J) & \mathbf{H}_k^{\text{ub}}(J-1) & \cdots & \mathbf{H}_k^{\text{ub}}(1) \end{bmatrix} \in \mathbb{C}^{JM \times J}, \quad (2)$$

where each block $\mathbf{H}_k^{\text{ub}}(j) = [h_{k,1}^{\text{ub}}(j), h_{k,2}^{\text{ub}}(j), \dots, h_{k,M}^{\text{ub}}(j)]^T \in \mathbb{C}^{M \times 1}$ is the channel at the j th tap. Similarly, the time-domain channel matrix between the k th user and the n th RIS element $\mathbf{H}_{k,n}^{\text{ur}} \in \mathbb{C}^{J \times J}$ is a circulant matrix, and the time-domain channel matrix between the n th RIS element and the BS $\mathbf{H}_n^{\text{rb}} \in \mathbb{C}^{JM \times J}$ is a block-circulant matrix. Let

$$\begin{aligned} \mathbf{r} &= [\mathbf{r}^T(1), \mathbf{r}^T(2), \dots, \mathbf{r}^T(J)]^T \in \mathbb{C}^{JM \times 1}, & \mathbf{r}(j) &= [r_1(j), r_2(j), \dots, r_M(j)]^T, \\ \mathbf{n} &= [\mathbf{n}^T(1), \mathbf{n}^T(2), \dots, \mathbf{n}^T(j)]^T \in \mathbb{C}^{JM \times 1}, & \mathbf{n}(j) &= [n_1(j), n_2(j), \dots, n_M(j)]^T. \end{aligned}$$

Then, the received baseband signal is given by

$$\mathbf{r} = \sum_{k=1}^K \left(\mathbf{H}_k^{\text{ub}} + \sum_{n=1}^N \theta_n \mathbf{H}_{k,n}^{\text{rb}} \mathbf{H}_{k,n}^{\text{ur}} \right) \mathbf{s}_k + \mathbf{n}. \quad (3)$$

The frequency-domain channel matrix \mathbf{G}_k^{ub} corresponding to \mathbf{H}_k^{ub} is a block-diagonal matrix given by

$$\mathbf{G}_k^{\text{ub}} = \begin{bmatrix} \mathbf{G}_k^{\text{ub}}(1) & \mathbf{0} & \cdots & \mathbf{0} \\ \mathbf{0} & \mathbf{G}_k^{\text{ub}}(2) & \ddots & \vdots \\ \vdots & \ddots & \ddots & \mathbf{0} \\ \mathbf{0} & \mathbf{0} & \cdots & \mathbf{G}_k^{\text{ub}}(J) \end{bmatrix} \in \mathbb{C}^{JM \times J} \quad (4a)$$

with its j th diagonal block calculated as

$$\mathbf{G}_k^{\text{ub}}(j) = \frac{1}{J} \sum_{l=1}^J \mathbf{H}_k^{\text{ub}}(l) \exp(-i2\pi j(l-1)/J), \quad (4b)$$

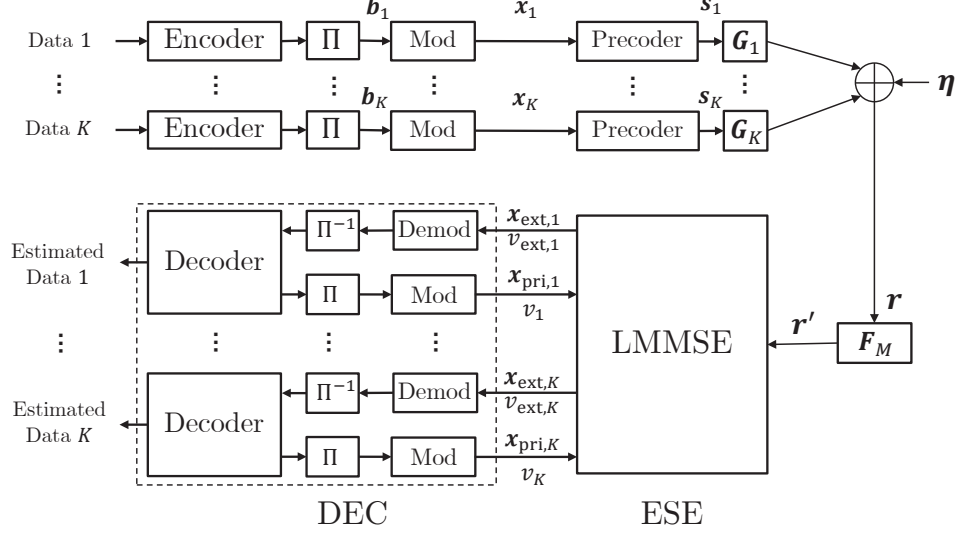


Fig. 2. The transmitter and (iterative) receiver structure for the uplink MIMO-NOMA system. The transmitter consists of an FEC encoder, an interleaver (denoted by Π), a modulator (denoted by Mod) and a linear precoder. The iterative receiver consists of a LMMSE-ESE module and a DEC module that handle the linear constraint and the coding constraint, respectively.

where $i = \sqrt{-1}$. A concise form of (4) is given by

$$\mathbf{G}_k^{\text{ub}} = \mathbf{F}_M \mathbf{H}_k^{\text{ub}} \mathbf{F}^H, \quad \mathbf{H}_k^{\text{ub}} = \mathbf{F}_M^H \mathbf{G}_k^{\text{ub}} \mathbf{F}, \quad (5)$$

where $\mathbf{F} \in \mathbb{C}^{J \times J}$ is the J -by- J unitary discrete Fourier transform (DFT) matrix, $\mathbf{F}_M = \mathbf{F} \otimes \mathbf{I}_M$ with \mathbf{I}_M being the $M \times M$ identity matrix. Similar to \mathbf{G}_k^{ub} , $\mathbf{G}_n^{\text{ur}} \in \mathbb{C}^{JM \times J}$ is a block-diagonal matrix with block-size M -by-1, and $\mathbf{G}_{k,n}^{\text{rb}} \in \mathbb{C}^{J \times J}$ is a diagonal matrix. After applying the DFT at the BS, we obtain the frequency-domain received signal as

$$\mathbf{r}' = \mathbf{F}_M \mathbf{r} = \sum_{k=1}^K \left(\mathbf{G}_k^{\text{ub}} + \sum_{n=1}^N \theta_n \mathbf{G}_{k,n}^{\text{rb}} \mathbf{G}_n^{\text{ur}} \right) \mathbf{F} \mathbf{s}_k + \boldsymbol{\eta}, \quad (6)$$

where $\boldsymbol{\eta} = \mathbf{F}_M \mathbf{n} \sim \mathcal{CN}(\mathbf{0}, \sigma^2 \mathbf{I})$ is an AWGN.

B. Transmitter Structure

The transmitter is illustrated at the upper part of Fig. 2. For each user k , its data is first encoded by forward-error-correction codes, such as the low-density parity-check (LDPC) code, with coding rate R_k , and then permuted by an interleaver to obtain $\mathbf{b}_k = [\mathbf{b}_{k,1}^T, \mathbf{b}_{k,2}^T, \dots, \mathbf{b}_{k,J}^T]^T$, where $\mathbf{b}_{k,j} \in \{0, 1\}^{Q_k}$ and Q_k is the number of bits per modulated symbol of user k . For simplicity, we assume that all the users adopt the same type of modulation, implying $Q_1 =$

$\dots = Q_K = Q$. The modulated vector $\mathbf{x}_k \in \mathbb{C}^{J \times 1}$ is generated by mapping each $\mathbf{b}_{k,j}$ to a discrete constellation $\mathcal{X}_k = \{c_{k,1}, c_{k,2}, \dots, c_{k,2^Q}\}$ with zero mean and unit variance. Then, \mathbf{x}_k is linearly precoded by [20]

$$\mathbf{s}_k = \mathbf{F}^H \mathbf{W}_k \mathbf{F} \mathbf{x}_k, \quad (7)$$

where $\mathbf{W}_k = \text{diag}\{W_k(1, 1), \dots, W_k(J, J)\}$ is used for power allocation among the subcarriers. Substituting (7) into (6), we obtain

$$\mathbf{r}' = \sum_{k=1}^K \left(\mathbf{G}_k^{\text{ub}} + \sum_{n=1}^N \theta_n \mathbf{G}_n^{\text{rb}} \mathbf{G}_{k,n}^{\text{ur}} \right) \mathbf{W}_k \mathbf{F} \mathbf{x}_k + \boldsymbol{\eta} \quad (8a)$$

$$= \sum_{k=1}^K \mathbf{G}_k(\boldsymbol{\theta}) \mathbf{W}_k \mathbf{F} \mathbf{x}_k + \boldsymbol{\eta}, \quad (8b)$$

where $\mathbf{G}_k(\boldsymbol{\theta}) = \mathbf{G}_k^{\text{ub}} + \sum_{n=1}^N \theta_n \mathbf{G}_n^{\text{rb}} \mathbf{G}_{k,n}^{\text{ur}}$ is the equivalent frequency-domain channel matrix, and $\boldsymbol{\theta} = [\theta_1, \dots, \theta_N]^T$.

C. Receiver Structure

The existing works on RIS mostly aim to improve the system performance by assuming an ideal receiver with capacity-achieving performance. Such a capacity-achieving receiver usually involves prohibitively high complexity. Instead, we here consider a low-complexity iterative receiver [20], which is meaningful for practical implementation.

As illustrated in the lower part of Fig. 2, the iterative receiver consists of an elementary signal estimator (ESE) that handles the linear constraint in (8b), and a generalized decoding processor (DEC) that handles the coding constraint [20]. The ESE and the DEC are executed iteratively.

1) *LMMSE-ESE Module*: The ESE carries out the linear minimum mean-square error (LMMSE) estimation based on the channel input \mathbf{r}' and the messages from the DEC $\{\mathbf{x}_{\text{pri},k}, v_k\}$. The signal \mathbf{x}_k is approximately modeled by a Gaussian distribution $\mathcal{CN}(\mathbf{x}_{\text{pri},k}, v_k \mathbf{I})$. Given \mathbf{r}' , the *a posteriori* covariance matrix and *a posteriori* mean of \mathbf{x}_k are expressed as [20]

$$\mathbf{V}_{\text{post},k} = v_k \mathbf{I} - v_k^2 \mathbf{A}_k^H \mathbf{V}^{-1} \mathbf{A}_k, \quad (9a)$$

$$\mathbf{x}_{\text{post},k} = \mathbf{x}_{\text{pri},k} + v_k \mathbf{A}_k^H \mathbf{V}^{-1} \left(\mathbf{r}' - \sum_{k'=1}^K \mathbf{A}_{k'} \mathbf{x}_{\text{pri},k'} \right), \quad (9b)$$

where

$$\mathbf{A}_k = \mathbf{G}_k(\boldsymbol{\theta}) \mathbf{W}_k \mathbf{F}, \quad (9c)$$

$$\mathbf{V} = \sum_{k'=1}^K v_{\text{pri},k'} \mathbf{A}_{k'} \mathbf{A}_{k'}^H + \sigma^2 \mathbf{I}. \quad (9d)$$

Following [29], we calculate the extrinsic variance and mean as the output of the LMMSE-ESE:

$$v_{\text{ext},k} = \left(v_{\text{post},k}^{-1} - v_k^{-1} \right)^{-1}, \quad (10a)$$

$$\mathbf{x}_{\text{ext},k} = v_{\text{ext},k} \left(v_{\text{post},k}^{-1} \mathbf{x}_{\text{post},k} - v_k^{-1} \mathbf{x}_{\text{pri},k} \right), \quad (10b)$$

where $v_{\text{post},k} = \frac{1}{J} \text{tr}\{\mathbf{V}_{\text{post},k}\}$. In (10), $\mathbf{x}_{\text{ext},k}$ is modeled as an AWGN observation of \mathbf{x}_k :

$$\mathbf{x}_{\text{ext},k} = \mathbf{x}_k + \boldsymbol{\xi}_k, \quad (11)$$

where $\boldsymbol{\xi}_k \sim \mathcal{CN}(\mathbf{0}, \rho_k^{-1} \mathbf{I})$ with $\rho_k = v_{\text{ext},k}^{-1}$ being the SINR of the effective channel in (11).

2) *DEC Module*: The DEC module is composed of *a posterior* probability (APP) decoders, de-interleavers/interleavers and soft demodulators/modulators for all the users. Given $\mathbf{x}_{\text{ext},k}$, the soft demodulator calculates the log-likelihood ratio (LLR) of each $\mathbf{b}_{k,j}(q)$ as

$$\lambda_{k,j}(q) = \ln \frac{p(b_{k,j}(q) = 0 | x_{\text{ext},k}(j))}{p(b_{k,j}(q) = 1 | x_{\text{ext},k}(j))}, \quad j = 1, 2, \dots, J, q = 1, 2, \dots, Q. \quad (12)$$

After de-interleaving, APP decoding and interleaving, the *a posterior* LLR for each $\mathbf{b}_{k,j}$ is obtained, denoted by $\gamma_{k,j}$. Then we update the mean and variance of each $x_{k,j}$:

$$\bar{x}_{k,j} = \mathbb{E}[x_{k,j} | \gamma_{k,j}] = \sum_{c_k \in \mathcal{X}_k} c_k p(x_{k,j} = c_k | \gamma_{k,j}), \quad (13a)$$

$$\bar{v}_k = \frac{1}{J} \sum_{j=1}^J \sum_{c_k \in \mathcal{X}_k} |c_k - \bar{x}_{k,j}|^2 p(x_{k,j} = c_k | \gamma_{k,j}). \quad (13b)$$

Similarly to (10a) and (10b), we update the *a priori* mean and variance of \mathbf{x}_k for the LMMSE-ESE by

$$v_k = \left(\bar{v}_k^{-1} - v_{\text{ext},k}^{-1} \right)^{-1}, \quad (14a)$$

$$\mathbf{x}_{\text{pri},k} = v_k \left(\bar{v}_k^{-1} \bar{\mathbf{x}}_k - v_{\text{ext},k}^{-1} \mathbf{x}_{\text{ext},k} \right). \quad (14b)$$

The remainder of this paper is devoted to the optimization of the system performance over the power allocation matrix $\{\mathbf{W}\}_k$ and the RIS phase shifts $\boldsymbol{\theta}$. This optimization can be done based on the well-known capacity region of the multiple access (MAC) channel, with the details given

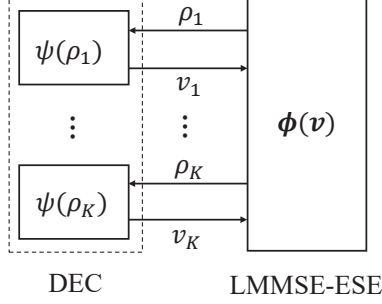


Fig. 3. An illustration of the overall evolution process of the iterative receiver. The LMMSE-ESE transfer function $\rho = \phi(v)$ is a vector function, and the DEC transfer function consists of K separable functions $v_k = \psi(\rho_k), \forall k$.

in Appendix A. However, there are two issues with this information-theoretic approach. First, the complexity of the formation-theoretic approach is exponential in the number of users (i.e., K), since the capacity region of a K -user MAC channel involves $2^K - 1$ rate constraints. Second, a practical iterative receiver may perform far away from the capacity due to implementation limitations. For example, with a limited computational power, the iterative receiver may strictly limit its iteration number in exchanging the messages between the ESE and the DEC. In this case, the optimization result based on information theory may be not a good choice for the practical system. For these reasons, we propose a state-evolution based optimization approach with lower complexity and better performance in the following section.

III. PERFORMANCE ANALYSIS

In this section, we describe the state evolution to characterize the performance of the iterative receiver, and then formulate the joint precoding and passive beamforming optimization problem. First, we provide the transfer functions of the DEC and the LMMSE-ESE, based on which the state evolution is established. Then, we formulate the joint optimization problem to reduce the total transmit power under the constraints of user BER and maximal iteration number.

A. State Evolution (SE)

The SE is a semi-analytical method for performance evaluation of an iterative receiver. Specifically, we use the output SINR $\rho = [\rho_1, \dots, \rho_K]^T$ to characterize the performance of the LMMSE-ESE, and the output variance $v = [v_1, \dots, v_K]^T$ to characterize the performance of the DEC,

while the output of a module is the input of the other module. As shown in Fig. 3, we track the performance by the following recursion: Start with $\mathbf{v}^{(0)} = [1, \dots, 1]^T$,

$$\boldsymbol{\rho}^{(t)} = \boldsymbol{\phi}(\mathbf{v}^{(t-1)}), \quad (15a)$$

$$\mathbf{v}^{(t)} = \boldsymbol{\psi}(\boldsymbol{\rho}^{(t)}), \quad (15b)$$

where the superscript $t = 1, 2, \dots, T$ is the iteration number with T being the maximum iteration number, the MIMO function $\boldsymbol{\rho} = \boldsymbol{\phi}(\mathbf{v})$ is the transfer function of the LMMSE-ESE, and the function $\mathbf{v} = \boldsymbol{\psi}(\boldsymbol{\rho})$ is the transfer function of the DEC, consisting of K separable single-input single-output (SISO) functions $v_k = \psi_k(\rho_k), k = 1, \dots, K$. We assume that the channel code of each user is identical to each other, and thus $\psi(\cdot) = \psi_1(\cdot) = \dots = \psi_K(\cdot)$.

We first describe the ESE transfer function $\boldsymbol{\phi}(\mathbf{v})$. Without loss of generality, denote $\boldsymbol{\phi}(\mathbf{v}) = [\phi_1(\mathbf{v}), \dots, \phi_K(\mathbf{v})]^T$. From (9), (10) and the definition $\rho_k = v_{\text{ext},k}^{-1}$ under (11), $\phi_k(\mathbf{v})$ can be expressed as

$$\rho_k = \phi_k(\mathbf{v}) = \frac{\tau_k}{1 - v_k \tau_k}, \quad (16a)$$

where

$$\tau_k = \frac{1}{J} \text{tr} \left\{ \mathbf{A}_k^H \left(\sum_{k'=1}^K v_{k'} [\mathbf{G}_{k'}(\boldsymbol{\theta}) \mathbf{W}_{k'}]^2 + \sigma^2 \mathbf{I} \right)^{-1} \mathbf{A}_k \right\}. \quad (16b)$$

Hence, $\phi_k(\cdot)$ is a function of $\{\mathbf{W}_k'\}$ and $\boldsymbol{\theta}$.

We now consider the DEC transfer function $\boldsymbol{\psi}(\boldsymbol{\rho})$. Since each user's data are decoded separately at the DEC, we can express $\boldsymbol{\psi}(\boldsymbol{\rho})$ as $\boldsymbol{\psi}(\boldsymbol{\rho}) = [\psi(\rho_1), \dots, \psi(\rho_K)]^T$, where $\psi(\cdot)$ is a monotone increasing function of the SINR ρ_k . $\psi(\cdot)$ can be numerically obtained by local Monte Carlo decoding by taking (11) as the input [20].

Denote by $P_{e,k}$ the BER of user k . Note that $P_{e,k} = \xi(v_k)$ is a monotone increasing function that maps the input of DEC v_k to the output BER $P_{e,k}$, where $\xi(\cdot)$ can be obtained by simulations similarly to $\psi(\cdot)$. Thus, the output BER at the last iteration is given by $\xi(v_k^{(T)})$. Given a target performance $P_{\text{tar},k}$, the required v_k can be calculated by $v_{\text{tar},k} = \xi^{-1}(P_{\text{tar},k})$, where $\xi^{-1}(\cdot)$ is the inverse of $\xi(\cdot)$. To achieve the target BER of each user, we have $\xi(v_k^{(T)}) \leq P_{\text{tar},k}, \forall k$, i.e.,

$$v_k^{(T)} \leq v_{\text{tar},k}, \quad \forall k. \quad (17)$$

We say that there exists a feasible path \mathcal{L} in the K -dimension variance space (v_1, \dots, v_K) from the initial point $(1, \dots, 1)$ to the target point $(v_{\text{tar},1}, \dots, v_{\text{tar},K})$ if (17) is met [24]. In other words, if (17) is met, there exists a curve \mathcal{L} starting from (v_1, \dots, v_K) and ending at $(v_{\text{tar},1}, \dots, v_{\text{tar},K})$

such that for each user k , the ESE transfer function $\phi_k(\mathbf{v})$ is above the inverse of the DEC transfer function $\psi(\rho_k)$, i.e.,

$$\phi_k(\mathbf{v}) > \psi^{-1}(v_k), \quad \forall k, \text{ for } \mathbf{v} \in \mathcal{L}. \quad (18)$$

Fig. 4 illustrates the path condition (17) in a two-user system. We see that there generally exists multiple potential paths that satisfy the path condition.

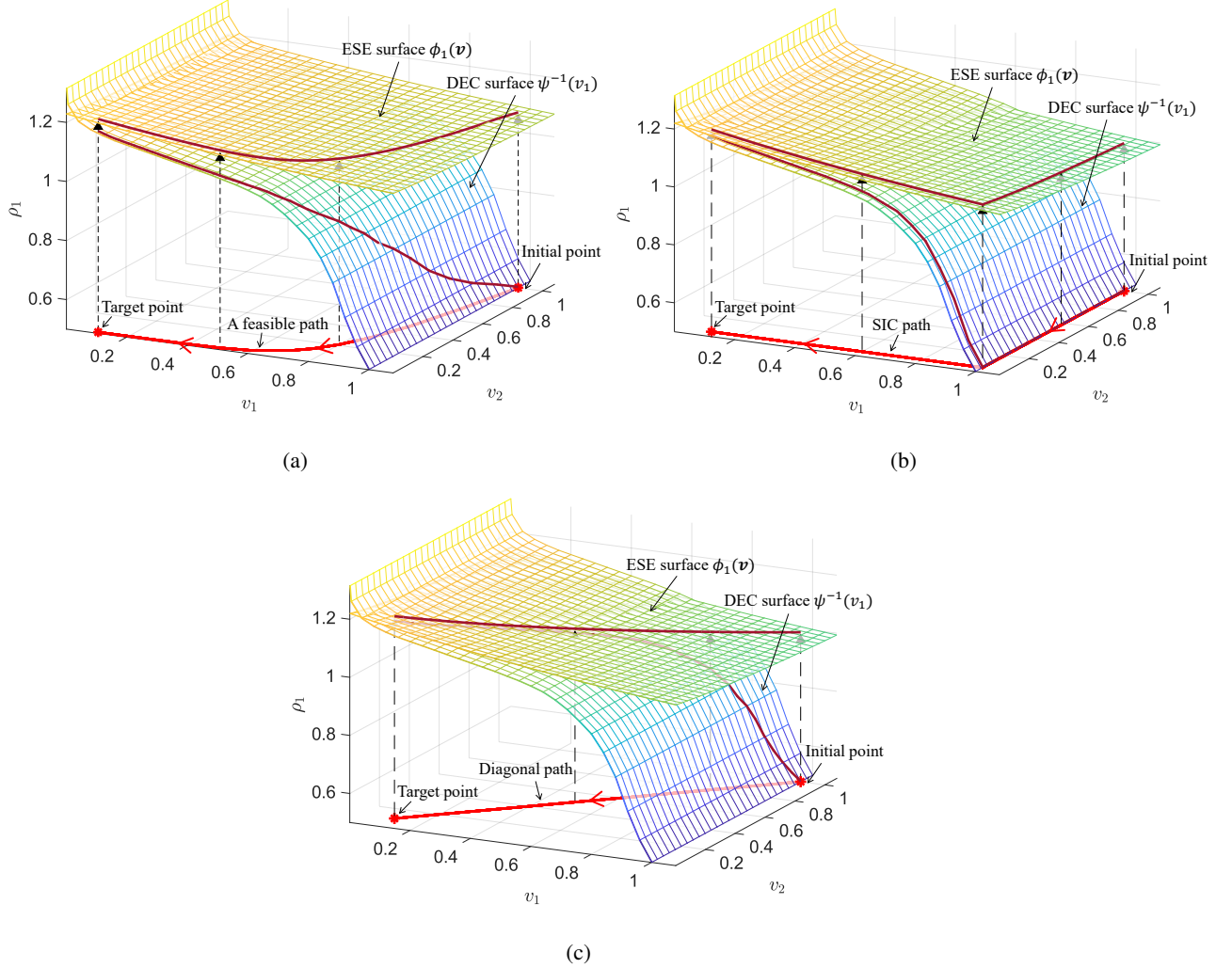


Fig. 4. Examples of the path condition (17) for user 1 in a 2-user system. (a) A feasible path. (b) The SIC path where the users are decoded one by one, which is a special case of the groupwise SIC in Section IV. (c) The diagonal path proposed in [24], where the input variances of the ESE are set to equal to each other. Thus, the corresponding path is the diagonal of the unit square (or equivalently, a two-dimensional unit cube) formed by the initial point $(1, 1)$ and the point $(0, 0)$.

B. Problem Formulation

We aim to jointly optimize $\{\mathbf{W}_k\}$, $\boldsymbol{\theta}$ and path \mathcal{L} to minimize the total transmit power for the iterative receiver under the constraints of target BER and maximum number of iterations. This problem can be formulated as

$$\mathcal{P}^{\text{lte}} : \min_{\{\mathbf{W}_k\}, \boldsymbol{\theta}, \mathcal{L}} \sum_{k=1}^K \sum_{j=1}^J |W_k(j, j)|^2 \quad (19a)$$

$$\text{s.t. } \phi_k(\mathbf{v}) > \psi^{-1}(v_k), \forall k, \text{ for } \mathbf{v} \in \mathcal{L}, \quad (19b)$$

$$T \leq T_{\max}, \quad (19c)$$

$$|\theta_n| = 1, \forall n, \quad (19d)$$

where (19b) is the target BER constraint from (18), (19c) the constraint of the maximal allowed iteration number T_{\max} , and (19d) the unit-modulus constraint of the RIS elements. In practice, T_{\max} is usually set to a small integer to reduce the computational complexity of the receiver.

It is generally difficult to find the globally optimal solution to \mathcal{P}^{lte} . On one hand, the unit-modulus constraint (19d) is non-convex, and so is the constraint (19b) as seen from (16). Therefore, \mathcal{P}^{lte} is a non-convex optimization program that is difficult to solve. On the other hand, the optimization result of $\{\mathbf{W}_k\}$ and $\boldsymbol{\theta}$ highly depends on the choice of the path \mathcal{L} , where \mathcal{L} is a curve starting from (v_1, \dots, v_K) and ending at $(v_{\text{tar},1}, \dots, v_{\text{tar},K})$. It is computationally infeasible to search over all the feasible paths in the K -dimension space [22], [24]. In [24], the authors proposed a diagonal path as shown in Fig. 4(c), where the input variances of the ESE are set to equal to each other. This is however far from optimal based on our experimental observations. In the next section, we provide an efficient path selection method to obtain an approximate solution to \mathcal{P}^{lte} .

IV. THE GROUPWISE SIC APPROACH

In this section, we present a groupwise-SIC approach for problem \mathcal{P}^{lte} . We start with the description of the groupwise SIC approach. Based on that, \mathcal{P}^{lte} is simplified and then solved by alternately optimizing precoding and passive beamforming.

A. Groupwise SIC

We first describe the groupwise SIC approach [30], a.k.a, sequential group detection [31], [32]. In the groupwise SIC, the users are divided into several groups, and are decoded and cancelled

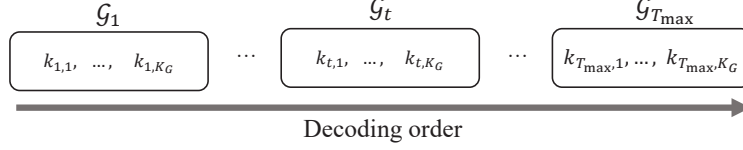


Fig. 5. The groupwise SIC approach. When decoding \mathcal{G}_t at the t th iteration, only the signals from \mathcal{G}_{t+1} to $\mathcal{G}_{T_{\max}}$ are regarded as interference, i.e., the interference from \mathcal{G}_1 to \mathcal{G}_{t-1} are assumed to be perfectly cancelled.

successively in a group-by-group manner. Following this idea, we divide the users into T_{\max} groups, and the users in group t are decoded (i.e., to achieve the target BER) at the t th iteration. Denote by $\mathcal{K} = \{1, \dots, K\}$ the total user set, and by $\mathcal{G}_t = \{k_{t,1}, k_{t,2}, \dots, k_{t,|\mathcal{G}_t|}\}$ the user set of group t . As shown in Fig. 5, the users are decoded in the order from \mathcal{G}_1 to $\mathcal{G}_{T_{\max}}$, and the interference from the decoded groups is assumed to be perfectly cancelled.

The optimal user grouping is generally difficult to determine. We will discuss how to find a sub-optimal user grouping strategy later in Section IV-D. Here we focus on the joint optimization of $\{\mathbf{W}\}$ and $\boldsymbol{\theta}$ for fixed user grouping $\{\mathcal{G}_t\}$. Given $\{\mathcal{G}_t\}$, \mathcal{P}^{lte} is reduced to

$$\mathcal{P}^{\text{SIC}} : \min_{\{\mathbf{W}_k\}, \boldsymbol{\theta}} \sum_{k=1}^K \sum_{j=1}^J |W_k(j, j)|^2 \quad (20a)$$

$$\text{s.t. } \phi'_k \geq \rho_{\text{tar},k}, \forall k, \quad (20b)$$

$$|\theta_n| = 1, \forall n. \quad (20c)$$

where

$$\rho_{\text{tar},k} = \psi^{-1}(v_{\text{tar},k}), \quad (20d)$$

$$\phi'_k = \frac{\tau'_k}{1 - \tau'_k}, \quad (20e)$$

$$\tau'_k = \frac{1}{J} \text{tr} \left\{ \mathbf{A}_k^H \left(\sum_{k' \in \bigcup_{t'=t}^{T_{\max}} \mathcal{G}_{t'}} [\mathbf{G}_{k'}(\boldsymbol{\theta}) \mathbf{W}_{k'}]^2 + \sigma^2 \mathbf{I} \right)^{-1} \mathbf{A}_k \right\}. \quad (20f)$$

Eq. (20b) is the user BER constraint, and (20c) is the RIS unit-modulus constraint. Different from (16b), for user k in group \mathcal{G}_t , the summation in (20f) contains the users from group \mathcal{G}_t to $\mathcal{G}_{T_{\max}}$ since the interference from the previous groups has been cancelled. Due to the non-convexity of (20b) and (20c), \mathcal{P}^{SIC} is non-convex and is hard to solve directly. In this paper, to obtain an approximate solution, we use the alternating optimization (AO) method to find a sub-optimal choice of $\{\mathbf{W}_k\}$ and $\boldsymbol{\theta}$.

B. Optimization of $\{\mathbf{W}_k\}$ Given $\boldsymbol{\theta}$

Given $\boldsymbol{\theta}$, \mathcal{P}^{SIC} in (19) is reduced to

$$\mathcal{P}_{1.1}^{\text{SIC}} : \min_{\{\mathbf{W}_k\}} \sum_{k=1}^K \sum_{j=1}^J |W_k(j, j)|^2 \quad (21a)$$

$$\text{s.t. } \phi'_k \geq \rho_{\text{tar},k}, \forall k. \quad (21b)$$

However, $\mathcal{P}_{1.1}^{\text{SIC}}$ is a non-convex optimization problem due to the fractions and matrix inversions involved in ϕ'_k . We employ the fractional programming (FP) [25] to replace (21b) with convex constraints. For user k in group t , let $\mathbf{w}_k = [W_k(1, 1), \dots, W_k(j, j)]^T$, $\mathbf{a}_k = \mathbf{G}_k \mathbf{w}_k$ and $\mathbf{B}_t = \sum_{k' \in \bigcup_{t'=t}^{T_{\max}} \mathcal{G}_{t'}} [\mathbf{G}_{k'} \mathbf{W}_{k'}]^2 + \sigma^2 \mathbf{I}$, and we rewrite τ'_k in (20f) as

$$\tau'_k = \frac{1}{J} \mathbf{a}_k^H \mathbf{B}_t^{-1} \mathbf{a}_k. \quad (22)$$

With (20e) and (22), constraint (21b) can be rewritten as

$$\mathbf{a}_k^H \mathbf{B}_t^{-1} \mathbf{a}_k \geq \frac{J \rho_{\text{tar},k}}{1 + \rho_{\text{tar},k}}, \forall k. \quad (23)$$

Then, by introducing auxiliary variables $\{\mathbf{y}_k \in \mathbb{C}^{J \times 1}\}$, we can convert $\mathcal{P}_{1.2}^{\text{SIC}}$ to

$$\mathcal{P}_{1.2}^{\text{SIC}} : \min_{\{\mathbf{W}_k, \mathbf{y}_k\}} \sum_{k=1}^K \sum_{j=1}^J |W_k(j, j)|^2 \quad (24a)$$

$$\text{s.t. } 2\text{Re}\{\mathbf{y}_k^H \mathbf{a}_k\} - \mathbf{y}_k^H \mathbf{B}_t \mathbf{y}_k \geq \frac{J \rho_{\text{tar},k}}{1 + \rho_{\text{tar},k}}, \forall k. \quad (24b)$$

The equivalence between $\mathcal{P}_{1.1}^{\text{SIC}}$ and $\mathcal{P}_{1.2}^{\text{SIC}}$ is obtained by [25, Theorem 2]. Then, we solve $\mathcal{P}_{1.2}^{\text{SIC}}$ by alternately optimizing $\{\mathbf{y}_k\}$ and $\{\mathbf{W}_k\}$ as follows.

- 1) Given $\{\mathbf{W}_k\}$, the optimal solution of \mathbf{y}_k is

$$\mathbf{y}_k = \mathbf{B}_t^{-1} \mathbf{a}_k. \quad (25)$$

Note that (24b) is equivalent to (23) by substituting (25) into (24b).

- 2) Given $\{\mathbf{y}_k\}$, constraint (24b) is convex [25]. Thus, $\mathcal{P}_{1.2}^{\text{SIC}}$ is convex and can be solved through convex optimization tools such as CVX [33] and interior-point method [34].

C. Optimization of θ Given $\{\mathbf{W}_k\}$

Given $\{\mathbf{W}_k\}$, \mathcal{P}^{SIC} in (19) is reduced to

$$\mathcal{P}_{2.1}^{\text{SIC}} : \min_{\theta} \sum_{k=1}^K \sum_{j=1}^J |W_k(j, j)|^2 \quad (26a)$$

$$\text{s.t. } \phi'_k \geq \rho_{\text{tar},k}, \forall k, \quad (26b)$$

$$|\theta_n| = 1, \forall n. \quad (26c)$$

In fact, $\mathcal{P}_{2.1}^{\text{SIC}}$ is a feasibility-check problem since the objective function is invariant to the optimization variable θ . To improve the optimization performance, we try to increase the minimum gap between ϕ'_k and $\rho_{\text{tar},k}$ by optimizing θ , which provides a wider feasible region of $\{\mathbf{W}_k\}$ for $\mathcal{P}_{1.1}^{\text{SIC}}$ at the next iteration and allows for further power reduction. Thus, we reformulate the problem as

$$\mathcal{P}_{2.2}^{\text{SIC}} : \max_{\theta} \min_k \phi'_k(\theta) - \rho_{\text{tar},k} \quad (27a)$$

$$\text{s.t. } |\theta_n| = 1, \forall n, \quad (27b)$$

where ϕ'_k is rewritten as $\phi'_k(\theta)$ to indicate that it is a function of θ . To deal with the non-convex unit-modulus constraint (27b), we replace θ_n by β_n , where $\theta_n = e^{j\beta_n}$ and $\beta_n \in \mathbb{R}, \forall n$. Let $\beta = [\beta_1, \dots, \beta_N]^T$, $\mathcal{P}_{2.2}^{\text{SIC}}$ is recast to

$$\mathcal{P}_{2.3}^{\text{SIC}} : \max_{\beta \in \mathbb{R}^N} \min_k \phi'_k(\beta) - \rho_{\text{tar},k}. \quad (28)$$

Then, by exploiting successive convex approximation (SCA), we solve a serial of surrogate problems to obtain a sub-optimal solution to $\mathcal{P}_{2.3}^{\text{SIC}}$ [35].

Lemma 1: The surrogate function

$$l_k(\beta, \bar{\beta}) \triangleq -\frac{\alpha_k(\bar{\beta})\kappa_k}{2} \|\beta - \bar{\beta}\|^2 + \alpha_k(\bar{\beta}) \nabla l'_k(\bar{\beta}, \bar{\beta})^T (\beta - \bar{\beta}) + C_k(\bar{\beta}) \quad (29)$$

satisfies

$$l_k(\bar{\beta}, \bar{\beta}) = \phi'_k(\bar{\beta}) - \rho_{\text{tar},k}, \quad (30a)$$

$$l_k(\beta, \bar{\beta}) \leq \phi'_k(\beta) - \rho_{\text{tar},k}, \quad (30b)$$

where κ_k is a constant no less than the Lipschitz constant of $\nabla l_k(\boldsymbol{\beta}, \bar{\boldsymbol{\beta}})$,

$$\alpha_k(\bar{\boldsymbol{\beta}}) = \frac{1}{J(1 - \tau'_k(\bar{\boldsymbol{\beta}}))^2}, \quad (31a)$$

$$C_k(\bar{\boldsymbol{\beta}}) = \phi'_k(\bar{\boldsymbol{\beta}}) - J\alpha_k(\bar{\boldsymbol{\beta}})\tau'_k(\bar{\boldsymbol{\beta}}) + \alpha_k(\bar{\boldsymbol{\beta}})l'_k(\bar{\boldsymbol{\beta}}, \bar{\boldsymbol{\beta}}) - \rho_{\text{tar},k}, \quad (31b)$$

$$l'_k(\boldsymbol{\beta}, \bar{\boldsymbol{\beta}}) = \frac{2}{J}\text{Re}\{\mathbf{y}_k(\bar{\boldsymbol{\beta}})^H \mathbf{a}_k(\boldsymbol{\beta})\} - \frac{1}{J}\mathbf{y}_k(\bar{\boldsymbol{\beta}})^H \mathbf{B}_k(\boldsymbol{\beta}) \mathbf{y}_k(\bar{\boldsymbol{\beta}}), \quad (31c)$$

and \mathbf{y}_k is given by (25).

The proof of Lemma 1 is given in Appendix B. Then, the surrogate problem is given by

$$\max_{\boldsymbol{\beta}} \min_k l_k(\boldsymbol{\beta}, \bar{\boldsymbol{\beta}}), \quad (32)$$

where $\bar{\boldsymbol{\beta}}$ is the optimization result of the previous surrogate problem. As pointed in [35], by solving a series of surrogate problems with the surrogate functions satisfying (30), we can obtain a stationary point of $\mathcal{P}_{2.3}^{\text{SIC}}$. Note that $l_k(\boldsymbol{\beta}, \bar{\boldsymbol{\beta}})$ is a concave function, and thus (32) can be easily solved by following [33], [34].

D. User Grouping

It is computationally involving to find the optimal user grouping with the minimal transmit power. Take exhaustive search for example, there are totally $(T_{\max})^K$ user groupings, and we need to solve the multiuser MIMO-OFDM power minimization problem for each user grouping. The complexity is prohibitively high in practice when K is large. In this paper, we provide a heuristic low-complexity user grouping strategy based on the sum rate maximization with fixed transmit power for each user.

We first evenly assign the users into T_{\max} groups as follows. Following [31], we order the users based on their channel conditions, where the users with relatively good channel conditions are decoded first, where the channel condition of each user is characterized by its achievable rate with groupwise SIC. For each group t , denote by $\mathcal{K}_t = \mathcal{K} - \sum_{t'=1}^{t-1} \mathcal{G}_{t'}$ the set consisting of users that are not in groups 1 to $t-1$, and set $\mathcal{K}_1 = \mathcal{K}$. Then, the achievable rate of user k in \mathcal{K}_t is given by [36]

$$R_{t,k} = \log \det \left(\mathbf{I} + \frac{1}{\sigma^2} \sum_{k' \in \mathcal{K}_t} [\mathbf{G}_{k'} \mathbf{W}_{k'}]^2 \right) - \log \det \left(\mathbf{I} + \frac{1}{\sigma^2} \sum_{k' \in \mathcal{K}_t, k' \neq k} [\mathbf{G}_{k'} \mathbf{W}_{k'}]^2 \right). \quad (33)$$

Clearly, the above rate $R_{t,k}$ of user k is obtained by assuming that the users in the first $t-1$ groups are already decoded and cancelled from the received signal, by following the groupwise

SIC strategy. We order the undecoded users by their achievable rates, and assign $T_G = K/T_{\max}$ users with the largest $R_{t,k}$ into \mathcal{G}_t . We sequentially determine the initial user grouping from \mathcal{G}_1 to $\mathcal{G}_{T_{\max}}$. The achievable sum rate is given by

$$R_{\text{sum}} = \sum_t \sum_{k \in \mathcal{G}_t} R_{t,k}. \quad (34)$$

Then, we adjust the user grouping to further increase the sum rate by reassigning each user to the preceding group or the subsequent group. Specifically, for user k assigned to group t , we calculate the sum rate after reassigning it to the preceding group as

$$R_{\text{sum}}^{\text{pre},k} = \begin{cases} R_{\text{sum}}, & t = 1, \\ \sum_{t'} \sum_{k' \in \mathcal{G}_{t'}^{\text{pre},k}} R_{t',k'}, & 1 < t \leq T_{\max}, \end{cases} \quad (35)$$

where $\{\mathcal{G}_{t'}^{\text{pre},k}\}_{t'=1}^{T_{\max}}$ is obtained from $\{\mathcal{G}_{t'}\}_{t'=1}^{T_{\max}}$ by reassigning user k to the preceding group $t-1$ for $1 < t \leq T_{\max}$. Similarly, the sum rate after reassigning user k to the subsequent group is given by

$$R_{\text{sum}}^{\text{sub},k} = \begin{cases} R_{\text{sum}}, & t = T_{\max}, \\ \sum_{t'} \sum_{k' \in \mathcal{G}_{t'}^{\text{sub},k}} R_{t',k'}, & 1 \leq t < T_{\max}, \end{cases} \quad (36)$$

where $\{\mathcal{G}_{t'}^{\text{sub},k}\}_{t'=1}^{T_{\max}}$ is obtained from $\{\mathcal{G}_{t'}\}_{t'=1}^{T_{\max}}$ by reassigning user k to the subsequent group $t+1$ for $1 \leq t < T_{\max}$. The overall user grouping strategy is summarized in Algorithm 1. We see that the sum rate is non-decreasing by adjusting the user grouping. The reassigning operation is repeated for all the users until the sum rate R_{sum} does not increase anymore. Since the sum rate is non-decreasing, the convergence of the above process is guaranteed.

E. Convergence and Complexity

The overall groupwise SIC approach is summarized in Algorithm 2. The convergence of the algorithm is guaranteed, since the objective function is non-increasing during the iteration of AO and is also lower-bounded by zero. The algorithm stops when the change of the objective function is less than a predetermined threshold. Using the interior-point method [37] for $\mathcal{P}_{1,2}^{\text{SIC}}$ and $\mathcal{P}_{2,3}^{\text{SIC}}$, the complexity of one iteration of Algorithm 2 is $\mathcal{O}((K(J+1))^{3.5} + T_1 N^{3.5})$, where T_1 is the number of successive convex approximation iterations. Compared with the information-theoretic approach in Appendix A, whose complexity is $\mathcal{O}((KJ+2^K)^{3.5} + (2^K)^{3.5}N)$, the groupwise SIC algorithm has a much lower complexity as the number of users increases.

Algorithm 1: User grouping algorithm

Input: $r', \theta, \{G_k^{\text{ub}}\}, \{G_n^{\text{rb}}\}, \{G_{k,n}^{\text{ur}}\}, \{W_k\}, T_{\max}$.

```

1 for  $t = 1, \dots, T_{\max}$  do
2   | Order the unassigned users by (33), and assign  $T_G$  users with the largest  $R_{t,k}$  into  $\mathcal{G}_t$ ;
3 end
4 Calculate the sum rate  $R_{\text{sum}}$  by (34);
5 while  $R_{\text{sum}}$  is increasing do
6   | for  $k = 1, \dots, K$  do
7     | Calculate  $R_{\text{sum}}^{\text{pre},k}$  and  $R_{\text{sum}}^{\text{sub},k}$ ;
8     | if  $R_{\text{sum}}^{\text{pre},k} > R_{\text{sum}}$  and  $R_{\text{sum}}^{\text{pre},k} \geq R_{\text{sum}}^{\text{sub},k}$  then
9       |    $\mathcal{G}_t = \mathcal{G}_t^{\text{pre},k}, \forall t$  and  $R_{\text{sum}} = R_{\text{sum}}^{\text{pre},k}$ ;
10    | end
11    | if  $R_{\text{sum}}^{\text{sub},k} > R_{\text{sum}}$  and  $R_{\text{sum}}^{\text{sub},k} > R_{\text{sum}}^{\text{pre},k}$  then
12      |    $\mathcal{G}_t = \mathcal{G}_t^{\text{sub},k}, \forall t$  and  $R_{\text{sum}} = R_{\text{sum}}^{\text{sub},k}$ ;
13    | end
14  | end
15 end

```

Output: $\{\mathcal{G}_t\}$.

Algorithm 2: Groupwise SIC optimization

Input: $r', \{G_k^{\text{ub}}\}, \{G_n^{\text{rb}}\}, \{G_{k,n}^{\text{ur}}\}$.

```

1 Randomly generate an independent realization of  $\theta$ ;
2 Obtain the user grouping  $\{\mathcal{G}_t\}$  by Algorithm 1;
3 while the stopping criterion is not met do
4   | Update  $\{W_k\}$  by solving  $\mathcal{P}_{1.2}^{\text{SIC}}$  through convex optimization tools given  $\theta$ ;
5   | Obtain  $\beta$  by solving  $\mathcal{P}_{2.3}^{\text{SIC}}$  given  $\{W_k\}$ , and then update  $\theta$  by  $\theta = e^{j\beta}$ ;
6 end

```

Output: $\{W_k\}$ and θ .

V. NUMERICAL RESULTS

In this section, we evaluate the proposed scheme with simulations. The metrics are the average BER of all the users, i.e., $\frac{1}{K} \sum_k P_{e,k}$, and the average transmit power defined as $P = \frac{1}{JK} \sum_k \sum_j |W(j, j)|^2$. Consider a three-dimensional coordinate system, where the BS is located at $(0, 0, 10)$, and the receiving antennas are a uniform linear array located on the x -axis with half-wavelength antenna spacing. The RIS, located at $(50, 50, 10)$, is a uniform planar array parallel to the $x - z$ plane with half-wavelength element spacing. The locations of the users are randomly and uniformly distributed in the horizontal rectangular area formed by the point $(60, 0, 1.5)$ and the point $(110, 50, 1.5)$. Following [11], we assume that the user-RIS and RIS-BS channels are both Rician fading distributed, where the large-scale pathlosses are $10^{-3}d^{-2}$ and $10^{-3}d^{-2.5}$, respectively, with d being the distance, and the Rician factors are both 10. The user-BS channels are Rayleigh fading with the large-scale pathloss $10^{-3}d^{-4}$. The numbers of the delay taps of these channels are $L_{ur} = 2$, $L_{rb} = 5$ and $L_{rb} = 6$, respectively. We assume that all the users use the same channel code. The target BER is set as 10^{-4} , and the LDPC code in 3GPP TR 38.212 [38] for QPSK modulation, code rate = $1/2$ and information length = 2112 is used for the channel code. Since each codeword of a user is transmitted over a single OFDM symbol, the number of subcarriers is $J = 2112$. In practice, for complexity consideration, it is not necessary to allocate a different power for every subcarrier. Thus, we downsample the frequency channel to J' subcarriers in power optimization, i.e., $\mathbf{G}_k(\boldsymbol{\theta}) \in \mathbb{C}^{JM \times 1}$ to $\mathbf{G}'_k(\boldsymbol{\theta}) \in \mathbb{C}^{J'M \times 1}$. Then, every J/J' subcarriers share the same power. We set $\sigma^2 = -105$ dBm, and all the results are averaged more than 200 independent channel realizations. With the transmitter and iterative receiver in Section II, the proposed groupwise-SIC approach is compared with the following four baseline approaches:

- 1) **No-RIS approach:** Obtain the optimized $\{\mathbf{W}_k\}$ by solving $\mathcal{P}_{1,1}^{\text{SIC}}$ in IV-B with given $\mathbf{G}_k(\boldsymbol{\theta}) = \mathbf{G}_k^{\text{ub}}$ and $T_{\max} = 1$.
- 2) **Random-phases approach:** Obtain the optimized $\{\mathbf{W}_k\}$ by solving $\mathcal{P}_{1,1}^{\text{SIC}}$ in IV-B with a randomly generated $\boldsymbol{\theta}$ and $T_{\max} = 1$.
- 3) **Information-theoretic approach:** The optimization approach in Appendix A, where the joint precoding and passive beamforming optimization problem under the constraint of capacity region is formulated. This optimization approach is inspired by the single-user optimization algorithm in [23].

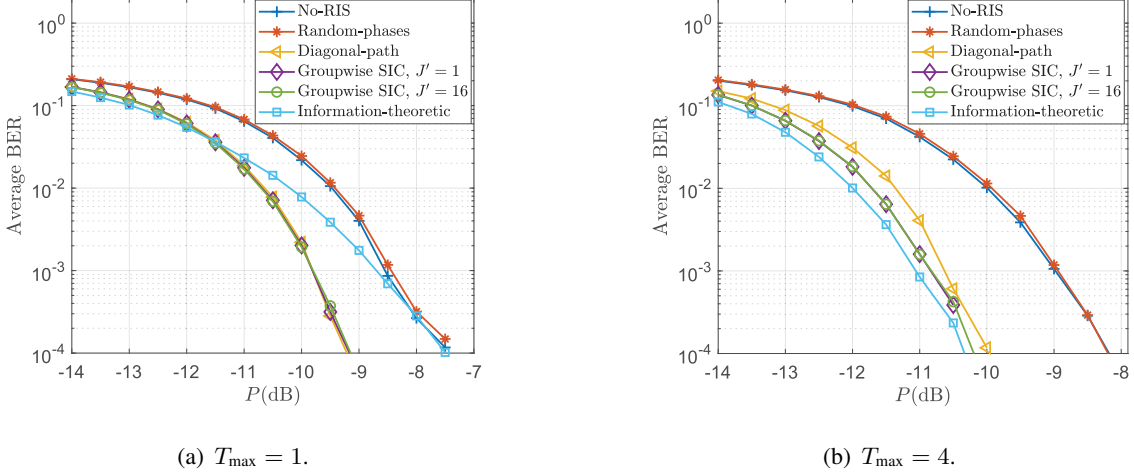


Fig. 6. Performance comparison between the proposed approach and baseline approaches. Settings: $K = 4, M = 8, N = 80$.

- 4) **Diagonal-path approach:** Using the diagonal path shown in Fig. 4(c) and removing the constraint of iteration number, Problem \mathcal{P}^{Ite} degenerates to the form similar to the single user optimization problem in [29], and can be solved using the FP and MM derived in this paper. However, the computational complexity of the diagonal-path approach is much higher than the groupwise SIC approach, since the number of constraints of the former one is much more due to the discretization of the path \mathcal{L} [24], [29]. Due to space limitations, the details of the diagonal-path approach are omitted.

We first evaluate the information-theoretic and other approaches in scenarios with a relatively small number of users (e.g., 4 users). In the following, the optimization approaches use $J' = 16$ unless specified otherwise, which means that every $2112/16 = 132$ subcarriers shares the same power. As shown in Fig. 6(a), we compare the proposed approaches and baseline approaches in a 4-user system with $T_{\max} = 1$. First, we see that the groupwise SIC approaches and the diagonal-path approach significantly outperform the other approaches, with about 1.5 dB power gain at the target BER. Second, the groupwise SIC approaches with $J' = 1$ and $J' = 16$ have almost the same performance. Fig. 6(a) shows the performance comparison between the approaches with $T_{\max} = 4$. The information-theoretic approach has a better performance than the other two approaches. The reason is that the iterative receiver with a higher complexity (or more iterations) behaves more like an ideal receiver, and so the information-theoretic approach works better. In addition, the diagonal-path approach has a performance gap less than 0.5 dB compared with other two optimization approaches.

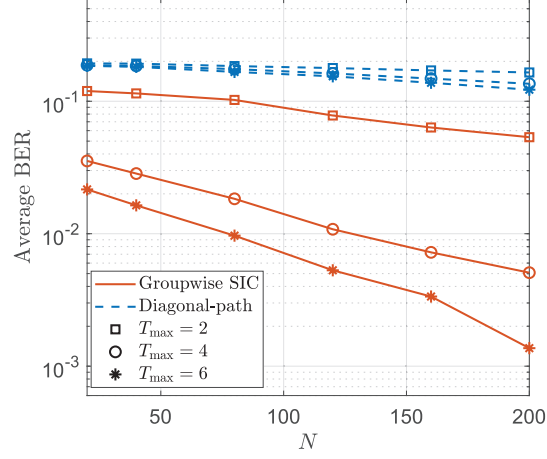


Fig. 7. Performance comparison under different numbers of RIS elements. Settings: $K = 12$ and $M = 8$.

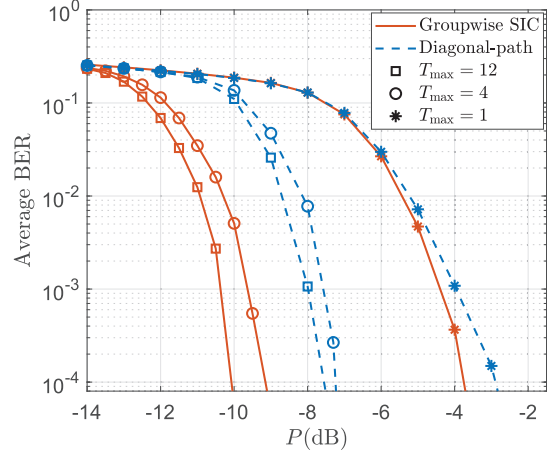


Fig. 8. Performance comparison under different maximum iteration numbers in a 12-user system. Settings: $M = 8$, and $N = 200$.

We now evaluate the groupwise SIC and diagonal-path approaches in the setting with more users (e.g., 4 to 16 users), where $J' = 1$ for all the approaches. Fig. 7 shows the performance comparison under different numbers of RIS elements N in a 12-user system. The groupwise SIC approach has a significant performance gain compared with the diagonal approach, no matter the maximum number of iterations is 2, 4 or 6. In addition, the performance of the groupwise SIC approach improves as the increasing of the iteration number T_{\max} , which provides a clear demonstration of the performance-complexity trade-off of our considered iterative detection scheme.

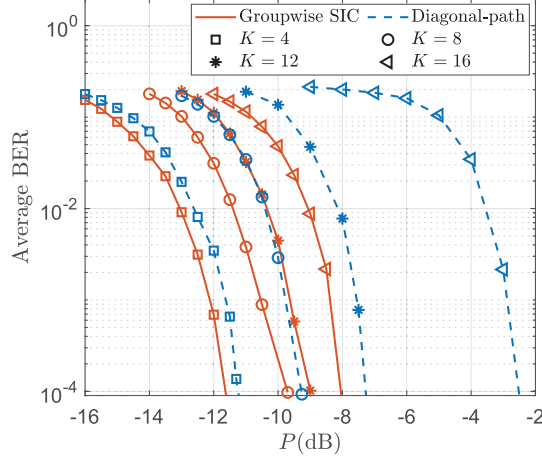


Fig. 9. Performance comparison with a varying number of users. Settings: $M = 8$, $N = 200$, and $T_{\max} = 4$.

The performances under different T_{\max} in a 12-user system are shown Fig. 8. First, we see that the groupwise SIC approach always outperforms the diagonal-path approach. As the number of iterations increases to 12, more than 2 dB power gain can be obtained. Second, with 4 iterations, a large portion of the performance gain can be obtained, which demonstrates the advantage of the groupwise SIC approach for a low-complexity receiver.

Fig. 9 shows the performance comparison under a varying number of users. The groupwise SIC approach shows a significant performance gain compared with the diagonal-path approach, especially when the number of users is large. The performance gain is less than 0.5 dB when $K = 4$, and increases to about 5 dB when $K = 16$. Therefore, it can be concluded that the groupwise SIC approach has advantages in both performance and computational complexity compared with its counterparts, especially when the number of iterations is relatively small.

VI. CONCLUSION

In this paper, we studied the RIS-aided multiuser MIMO-OFDM system with a specific iterative receiver. We formulated the joint optimization problem for the iterative receiver under the constraints of user BER and maximal iteration number. We proposed the low-complexity groupwise SIC approach and converted the problem to two sub-problems of precoding and passive beamforming. For precoding, we apply the FP to deal with the non-convex constraints with matrix inversion and fractions. For passive beamforming, we redesign the feasibility-check problem, and resort to the SCA to deal with the unit-modulus constraints of RIS. We also

provided a heuristic and low-complexity user grouping approach. We show that the proposed groupwise SIC approach has a much lower complexity than the information-theoretic approach. Numerical simulations showed that the groupwise SIC approach outperforms the information-theoretic approach and the diagonal-path approach, especially when the iteration number of the receiver is limited to a relatively small value.

APPENDIX A

INFORMATION-THEORETIC APPROACH

A. Problem Formulation

Denote by $\mathcal{K} = \{1, \dots, K\}$ the total user set. Following [36] and [39], the capacity region of the considered multiuser MIMO-OFDM transmission can be expressed as

$$\sum_{k \in \mathcal{K}_u} QR_k \leq \frac{1}{J + L_{\text{cp}}} \log \det \left(\mathbf{I} + \frac{1}{\sigma^2} \sum_{k \in \mathcal{K}_u} [\mathbf{G}_k(\boldsymbol{\theta}) \mathbf{W}_k]^2 \right), \mathcal{K}_u \subseteq \mathcal{K}, \quad (37)$$

where QR_k is the transmission rate per channel use. Then, the information-theoretic optimization problem is formulated by

$$\mathcal{P}^{\text{Info}} : \min_{\{\mathbf{W}_k\}, \boldsymbol{\theta}} \sum_{k=1}^K \sum_{j=1}^J |W_k(j, j)|^2 \quad (38a)$$

$$\text{s.t.} \quad \sum_{k \in \mathcal{K}_u} (J + L_{\text{cp}}) QR_k \leq \log \det \left(\mathbf{I} + \frac{1}{\sigma^2} \sum_{k \in \mathcal{K}_u} [\mathbf{G}_k(\boldsymbol{\theta}) \mathbf{W}_k]^2 \right), \mathcal{K}_u \subseteq \mathcal{K}, \quad (38b)$$

$$|\theta_n| = 1, \forall n. \quad (38c)$$

where (38a) is the total transmit power of all users, (38b) is the capacity region constraint, and (38c) is the unit-modulus constraint of the RIS's elements. As inspired by [23], we resort to the AO method to obtain an approximate solution to $\mathcal{P}^{\text{Info}}$ by optimizing $\{\mathbf{W}_k\}$ and each θ_n alternately, as described in the following subsections.

B. Optimization of $\{\mathbf{W}_k\}$ Given $\boldsymbol{\theta}$

Given $\boldsymbol{\theta}$, $\mathcal{P}^{\text{Info}}$ is reduced to

$$\mathcal{P}_1^{\text{Info}} : \min_{\{\mathbf{W}_k\}} \sum_{k=1}^K \sum_{j=1}^J |W_k(j, j)|^2 \quad (39a)$$

$$\text{s.t.} \quad \sum_{k \in \mathcal{K}_u} (J + L_{\text{cp}}) QR_k \leq \log_2 \det \left(\mathbf{I} + \frac{1}{\sigma^2} \sum_{k \in \mathcal{K}_u} [\mathbf{G}_k(\boldsymbol{\theta}) \mathbf{W}_k]^2 \right), \mathcal{K}_u \subseteq \mathcal{K}. \quad (39b)$$

Since $\log \det(\cdot)$ is a concave function of $\{\mathbf{W}_k\}$ [36], constraint (38b) is convex. Therefore, $\mathcal{P}_1^{\text{Info}}$ can be solved by the existing convex optimization tools [33], [34].

C. Optimization of θ_n Given $\{\mathbf{W}_k\}$ and $\{\theta_{n'}, n' \neq n\}$

Given $\{\mathbf{W}_k\}$ and $\{\theta_{n'}, n' \neq n\}$, $\mathcal{P}^{\text{Info}}$ is reduced to

$$\mathcal{P}_{2.1}^{\text{Info}} : \min_{\theta_n} \sum_{k=1}^K \sum_{j=1}^J |W_k(j, j)|^2 \quad (40a)$$

$$\text{s.t.} \quad \sum_{k \in \mathcal{K}_u} (J + L_{\text{cp}}) Q R_k \leq \log_2 \det \left(\mathbf{I} + \frac{1}{\sigma^2} \sum_{k \in \mathcal{K}_u} [\mathbf{G}_k(\boldsymbol{\theta}) \mathbf{W}_k]^2 \right), \mathcal{K}_u \subseteq \mathcal{K}, \quad (40b)$$

$$|\theta_n| = 1. \quad (40c)$$

Note that $\mathcal{P}_{2.1}^{\text{Info}}$ is a feasibility-check problem. Similar to $\mathcal{P}_{2.1}^{\text{SIC}}$ in Section IV-C, by introducing an auxiliary variable ΔR , we reformulate $\mathcal{P}_{2.1}^{\text{Info}}$ as

$$\mathcal{P}_{2.2}^{\text{Info}} : \max_{\theta_n, \Delta R} \Delta R \quad (41a)$$

$$\text{s.t.} \quad \sum_{k \in \mathcal{K}_u} Q(J + L_{\text{cp}})(R_k + \Delta R) \leq \log_2 \det \left(\mathbf{I} + \frac{1}{\sigma^2} \sum_{k \in \mathcal{K}_u} [\mathbf{G}_k(\boldsymbol{\theta}) \mathbf{W}_k]^2 \right), \mathcal{K}_u \subseteq \mathcal{K}, \quad (41b)$$

$$|\theta_n| = 1. \quad (41c)$$

To solve this problem, we rewrite $\mathbf{G}_k(\boldsymbol{\theta})$ as

$$\mathbf{G}_k(\boldsymbol{\theta}) = \mathbf{G}'_{n,k} + \theta_n \mathbf{G}_n^{\text{rb}} \mathbf{G}_{k,n}^{\text{ur}}, \quad (42)$$

where $\mathbf{G}'_{n,k} = \mathbf{G}_k^{\text{ub}} + \sum_{n' \neq n} \theta_{n'} \mathbf{G}_{n'}^{\text{rb}} \mathbf{G}_{k,n'}^{\text{ur}}$. As such, the right-hand side of (41b) can be rewritten as [23]

$$C_u(\theta_n) = \log_2 \det \left(\mathbf{I} + \frac{1}{\sigma^2} \sum_{k \in \mathcal{K}_u} \left(2\text{Re}\{\theta_n \mathbf{G}_n^{\text{rb}} \mathbf{G}_{k,n}^{\text{ur}} \mathbf{W}_k (\mathbf{W}_k \mathbf{G}'_{n,k})^H\} + [\mathbf{W}_k \mathbf{G}'_{n,k}]^2 + [\mathbf{G}_n^{\text{rb}} \mathbf{G}_{k,n}^{\text{ur}} \mathbf{W}_k]^2 \right) \right), \quad (43)$$

Then we apply the convex relaxation technique by relaxing $|\theta_n| = 1$ to $|\theta_n| \leq 1$. Thus, $\mathcal{P}_{2.2}^{\text{Info}}$ is converted to

$$\mathcal{P}_{2.3}^{\text{Info}} : \max_{\theta_n, \Delta R} \Delta R \quad (44a)$$

$$\text{s.t.} \quad \sum_{k \in \mathcal{K}_u} Q(J + L_{\text{cp}})(R_k + \Delta R) \leq C_u(\theta_n), \mathcal{K}_u \subseteq \mathcal{K}, \quad (44b)$$

$$|\theta_n| \leq 1. \quad (44c)$$

Since (44a)-(44c) are all convex, $\mathcal{P}_{2.3}^{\text{Info}}$ is a convex optimization problem that can be solved by existing convex optimization tools [33], [34]. During the iteration of AO, if the obtained θ_n for $\mathcal{P}_{2.3}^{\text{Info}}$ does not satisfy the constraint in (41b), we normalize θ_n by $\theta_n/|\theta_n|$ and then optimize $\{\mathbf{W}_k\}$ based on the normalized $\boldsymbol{\theta}$. As stated in [23], due to the above relaxation and normalization of $\boldsymbol{\theta}_n$, the convergence of the AO is not guaranteed.

D. Complexity

The numbers of constraints in (38b) and (44b) are both about 2^K . With the interior-point method [37], the complexity of one iteration is $\mathcal{O}((KJ+2^K)^{3.5}+(2^K)^{3.5}N)$, where the complexity of solving the $\mathcal{P}_1^{\text{Info}}$ and $\mathcal{P}_{2.3}^{\text{Info}}$ is $\mathcal{O}((KJ+2^K)^{3.5})$ and $\mathcal{O}((2^K)^{3.5})$, respectively.

APPENDIX B

PROOF OF LEMMA 1

We construct $l_k(\boldsymbol{\beta}, \bar{\boldsymbol{\beta}})$ by using the following three steps.

- 1) Lower bound $l_{1,k}(\boldsymbol{\beta}, \bar{\boldsymbol{\beta}})$ of ϕ'_k : Note that $\phi'_k = \frac{\tau'_k}{1-\tau'_k}$ is a convex function of τ'_k . Thus, the first order Taylor expansion of $\phi'_k(\tau'_k(\boldsymbol{\beta}))$ at $\tau'_k(\bar{\boldsymbol{\beta}})$ satisfies

$$l_{1,k}(\boldsymbol{\beta}, \bar{\boldsymbol{\beta}}) = \phi'_k(\bar{\boldsymbol{\beta}}) + \frac{\tau'_k(\boldsymbol{\beta}) - \tau'_k(\bar{\boldsymbol{\beta}})}{(1 - \tau'_k(\bar{\boldsymbol{\beta}}))^2} \leq \phi'_k(\boldsymbol{\beta}). \quad (45)$$

- 2) Lower bound $l_{2,k}(\boldsymbol{\beta}, \bar{\boldsymbol{\beta}})$ of $\tau'_k(\boldsymbol{\beta})$: With (25) in Section IV-B, we have $\mathbf{y}_k(\bar{\boldsymbol{\beta}}) = \mathbf{B}_t^{-1}(\bar{\boldsymbol{\beta}})\mathbf{a}_k(\bar{\boldsymbol{\beta}})$ and $\tau'_k(\boldsymbol{\beta}) = \frac{1}{J}\mathbf{a}_k^H(\boldsymbol{\beta})\mathbf{B}_t^{-1}(\boldsymbol{\beta})\mathbf{a}_k(\boldsymbol{\beta})$. From [25, Theorem 2], we obtain

$$\begin{aligned} l_{2,k}(\boldsymbol{\beta}, \bar{\boldsymbol{\beta}}) &= \frac{2}{J}\text{Re}\{\mathbf{y}_k^H(\bar{\boldsymbol{\beta}})\mathbf{a}_k(\boldsymbol{\beta})\} - \frac{1}{J}\mathbf{y}_k^H(\bar{\boldsymbol{\beta}})\mathbf{B}_k(\boldsymbol{\beta})\mathbf{y}_k(\bar{\boldsymbol{\beta}}) \\ &= \frac{2}{J}\text{Re}\{\mathbf{u}_k^H(\bar{\boldsymbol{\beta}})e^{j\beta}\} - \frac{1}{J}(e^{j\beta})^H\mathbf{U}_k(\bar{\boldsymbol{\beta}})e^{j\beta} + C_{1,k}(\bar{\boldsymbol{\beta}}) \\ &\leq \tau'_k(\boldsymbol{\beta}), \end{aligned} \quad (46a)$$

where

$$\mathbf{Y}_k(\bar{\boldsymbol{\beta}}) = \text{diag}\{\mathbf{y}_k(\bar{\boldsymbol{\beta}})\}, \quad (46b)$$

$$\mathbf{u}_k(\bar{\boldsymbol{\beta}}) = \mathbf{G}_{r,k}^H \mathbf{W}_k \otimes \mathbf{I}_M \mathbf{y}_k(\bar{\boldsymbol{\beta}}) - \sum_{k' \in \bigcup_{t'=t}^T \mathcal{G}_t} v_{k'} \mathbf{G}_{r,k'}^H \mathbf{Y}_k(\bar{\boldsymbol{\beta}}) \mathbf{W}_{k'} \mathbf{W}_{k'}^H \mathbf{G}_{d,k'}^T (\mathbf{y}_k^T(\bar{\boldsymbol{\beta}}))^H, \quad (46c)$$

$$\mathbf{U}_k(\bar{\boldsymbol{\beta}}) = \sum_{k' \in \bigcup_{t'=t}^T \mathcal{G}_t} v_{k'} \mathbf{G}_{r,k'}^H \mathbf{Y}_k(\bar{\boldsymbol{\beta}}) \mathbf{W}_{k'} \mathbf{W}_{k'}^H \mathbf{Y}_k(\bar{\boldsymbol{\beta}}) \mathbf{G}_{d,k'}, \quad (46d)$$

$$C_{1,k}(\bar{\beta}) = 2\text{Re}\{\mathbf{y}_k^H(\bar{\beta})\mathbf{G}_{d,k}\mathbf{w}_k\} - \sum_{k' \in \bigcup_{t'=t}^T \mathcal{G}_t} v_{k'} \mathbf{y}_k^H(\bar{\beta}) \mathbf{G}_{r,k'} \mathbf{W}_{k'} \mathbf{W}_{k'}^H \mathbf{G}_{d,k'}^H \mathbf{Y}_k(\bar{\beta}) - \sigma^2 \mathbf{y}_k^H(\bar{\beta}) \mathbf{y}_k(\bar{\beta}). \quad (46e)$$

3) Lower bound $l_{3,k}(\beta, \bar{\beta})$ of $l_{2,k}(\beta, \bar{\beta})$: We use the second order Taylor expansion as the lower bound of $l_{2,k}(\beta, \bar{\beta})$:

$$l_{3,k}(\beta, \bar{\beta}) = l_{2,k}(\bar{\beta}, \bar{\beta}) + \nabla l_{2,k}(\bar{\beta}, \bar{\beta})^T (\beta - \bar{\beta}) - \frac{\kappa_k}{2} \|\beta - \bar{\beta}\|_2^2 \leq l_{2,k}(\beta, \bar{\beta}) \quad (47)$$

where $\nabla l_{2,k}(\bar{\beta}, \bar{\beta}) = 2\text{Re}\{i\bar{\theta}^* \odot (\mathbf{U}_k \bar{\theta} - \mathbf{u}_k)\}$ is the gradient [40], and κ_k is a constant on less than the Lipschitz constant of $\nabla l_{2,k}(\beta, \bar{\beta})$ [35]. Note that κ_k can be chosen as follows. The gradient and the Hessian matrix of $l_{2,k}(\beta, \bar{\beta})$ are respectively given by

$$\nabla l_{2,k}(\beta, \bar{\beta}) = 2\text{Re}\{i(e^{i\beta})^* \odot (\mathbf{U}_k(\bar{\beta})e^{i\beta} - \mathbf{u}_k(\bar{\beta}))\}, \quad (48a)$$

$$\nabla^2 l_{2,k}(\beta, \bar{\beta}) = 2\text{Re}\left\{\begin{bmatrix} (e^{i\beta_1})^* \alpha_{k,1} \\ \vdots \\ (e^{i\beta_N})^* \alpha_{k,N} \end{bmatrix}\right\}, \quad (48b)$$

where

$$\alpha_{k,1} = \left[u_{k,1} - \sum_{n \neq 1} U_{k,1,n} e^{i\beta_n}, U_{k,1,2} e^{i\beta_2}, \dots, U_{k,1,N} e^{i\beta_N} \right], \quad (48c)$$

$$\alpha_{k,N} = \left[U_{k,N,1} e^{i\beta_1}, U_{k,N,2} e^{i\beta_2}, \dots, u_{k,N} - \sum_{n \neq N} U_{k,N,n} e^{i\beta_n} \right], \quad (48d)$$

$u_{k,n}$ is the n th element of $\mathbf{u}_k(\bar{\beta})$, and $U_{k,n,m}$ is the (n, m) th element of $\mathbf{U}_k(\bar{\beta})$. Note that $\|\nabla^2 l_{2,k}(\beta, \bar{\beta})\|_F$ is upper bounded by $\|\Gamma_k\|_F$, where

$$\Gamma_k = \begin{bmatrix} |u_{k,1}| + \sum_{n \neq 1} |U_{k,1,n}| & |U_{k,1,2}| & \cdots & |U_{k,1,N}| \\ |U_{k,2,1}| & |u_{k,2}| + \sum_{n \neq 2} |U_{k,2,n}| & \cdots & |U_{k,2,N}| \\ \vdots & \vdots & \ddots & \vdots \\ |U_{k,N,1}| & |U_{k,N,2}| & \cdots & |u_{k,N}| + \sum_{n \neq N} |U_{k,N,n}| \end{bmatrix}. \quad (49)$$

Then, we obtain

$$\|\nabla l_{2,k}(\beta_1, \bar{\beta}) - \nabla l_{2,k}(\beta_2, \bar{\beta})\|_2 \leq \|\Gamma_k\|_F \|\beta_1 - \beta_2\|_2, \quad (50)$$

which can be derived by using the mean value theorem for vector-valued functions. Thus, $\nabla l_{2,k}(\beta, \bar{\beta})$ is Lipschitz-continuous, where the Lipschitz constant L satisfies $L \leq \|\Gamma_k\|_F$. By simply setting $\kappa_k = \|\Gamma_k\|_F$, we obtain (47) [35].

Combining (45), (46) and (47), we obtain the lower bound of $\phi'_k(\beta) - \rho_{\text{tar},k}$:

$$l_k(\beta, \bar{\beta}) = -\frac{\alpha_k(\bar{\beta})\kappa_k}{2}\|\beta - \bar{\beta}\|^2 + \alpha_k(\bar{\beta})\nabla l_{2,k}(\bar{\beta}, \bar{\beta})^T(\beta - \bar{\beta}) + C_k(\bar{\beta}), \quad (51a)$$

where

$$\alpha_k(\bar{\beta}) = \frac{1}{J(1 - \tau'_k(\bar{\beta}))^2}, \quad (51b)$$

$$C_k(\bar{\beta}) = \phi'_k(\bar{\beta}) - J\alpha_k(\bar{\beta})\tau'_k(\bar{\beta}) + \alpha_k(\bar{\beta})l_{2,k}(\bar{\beta}, \bar{\beta}) - \rho_{\text{tar},k}. \quad (51c)$$

Thus, Lemma 1 holds by letting $l_{2,k}(\beta, \bar{\beta}) = l'_k(\beta, \bar{\beta})$ in (51).

REFERENCES

- [1] M. Di Renzo, M. Debbah, D.-T. Phan-Huy, A. Zappone, M.-S. Alouini, C. Yuen, V. Sciancalepore, G. C. Alexandropoulos, J. Hoydis, H. Gacanin *et al.*, “Smart radio environments empowered by reconfigurable AI meta-surfaces: An idea whose time has come,” *EURASIP J. Wirel. Commun. and Netw.*, May 2019.
- [2] Q. Wu and R. Zhang, “Towards smart and reconfigurable environment: Intelligent reflecting surface aided wireless network,” *IEEE Commun. Mag.*, vol. 58, no. 1, pp. 106–112, Nov. 2020.
- [3] L. You, J. Xiong, D. W. K. Ng, C. Yuen, W. Wang, and X. Gao, “Energy efficiency and spectral efficiency tradeoff in RIS-aided multiuser MIMO uplink transmission,” *IEEE Trans. Signal Process.*, vol. 69, pp. 1407–1421, 2021.
- [4] C. Huang, A. Zappone, G. C. Alexandropoulos, M. Debbah, and C. Yuen, “Reconfigurable intelligent surfaces for energy efficiency in wireless communication,” *IEEE Trans. Wireless Commun.*, vol. 18, no. 8, pp. 4157–4170, Aug. 2019.
- [5] L. You, J. Xiong, Y. Huang, D. W. K. Ng, C. Pan, W. Wang, and X. Gao, “Reconfigurable intelligent surfaces-assisted multiuser MIMO uplink transmission with partial CSI,” *IEEE Trans. Wireless Commun.*, vol. 20, no. 9, pp. 5613–5627, Sept. 2021.
- [6] S. Zhou, W. Xu, K. Wang, M. Di Renzo, and M.-S. Alouini, “Spectral and energy efficiency of IRS-assisted MISO communication with hardware impairments,” *IEEE Wireless Commun. Lett.*, vol. 9, no. 9, pp. 1366–1369, Sept. 2020.
- [7] F. Fang, Y. Xu, Q.-V. Pham, and Z. Ding, “Energy-efficient design of IRS-NOMA networks,” *IEEE Trans. Veh. Technol.*, vol. 69, no. 11, pp. 14 088–14 092, Nov. 2020.
- [8] S. Zhang and R. Zhang, “Capacity characterization for intelligent reflecting surface aided MIMO communication,” *IEEE J. Sel. Areas Commun.*, vol. 38, no. 8, pp. 1823–1838, Aug. 2020.
- [9] Q. Tao, J. Wang, and C. Zhong, “Performance analysis of intelligent reflecting surface aided communication systems,” *IEEE Commun. Lett.*, vol. 24, no. 11, pp. 2464–2468, Nov. 2020.
- [10] D. Li, “Ergodic capacity of intelligent reflecting surface-assisted communication systems with phase errors,” *IEEE Commun. Lett.*, vol. 24, no. 8, pp. 1646–1650, Aug. 2020.
- [11] G. Yang, X. Xu, Y. C. Liang, and M. Di Renzo, “Reconfigurable intelligent surface assisted non-orthogonal multiple access,” *IEEE Trans. Wireless Commun.*, vol. 20, no. 5, pp. 3137–3151, May 2021.
- [12] Y. Li, M. Jiang, Q. Zhang, and J. Qin, “Joint beamforming design in multi-cluster MISO NOMA reconfigurable intelligent surface-aided downlink communication networks,” *IEEE Trans. Commun.*, vol. 69, no. 1, pp. 664–674, Jan. 2021.
- [13] M. Fu, Y. Zhou, Y. Shi, and K. B. Letaief, “Reconfigurable intelligent surface empowered downlink non-orthogonal multiple access,” *IEEE Trans. Commun.*, vol. 69, no. 6, pp. 3802–3817, June 2021.

- [14] H. Guo, Y. Liang, J. Chen, and E. G. Larsson, "Weighted sum-rate maximization for reconfigurable intelligent surface aided wireless networks," *IEEE Trans. Wireless Commun.*, vol. 19, no. 5, pp. 3064–3076, May 2020.
- [15] S. Hu, Z. Wei, Y. Cai, D. W. K. Ng, and J. Yuan, "Sum-rate maximization for multiuser MISO downlink systems with self-sustainable IRS," in *Proc. IEEE GLOBECOM*, Dec. 2020, pp. 1–7.
- [16] Y. Xiu, J. Zhao, W. Sun, M. D. Renzo, G. Gui, Z. Zhang, and N. Wei, "Reconfigurable intelligent surfaces aided mmwave NOMA: Joint power allocation, phase shifts, and hybrid beamforming optimization," *IEEE Trans. Wireless Commun.*, vol. 20, no. 12, pp. 8393–8409, Dec. 2021.
- [17] Y. Xiu, J. Zhao, E. Basar, M. D. Renzo, W. Sun, G. Gui, and N. Wei, "Uplink achievable rate maximization for reconfigurable intelligent surface aided millimeter wave systems with resolution-adaptive ADCs," *IEEE Wireless Commun. Lett.*, vol. 10, no. 8, pp. 1608–1612, Aug. 2021.
- [18] Z. Li, M. Hua, Q. Wang, and Q. Song, "Weighted sum-rate maximization for multi-IRS aided cooperative transmission," *IEEE Wireless Commun. Lett.*, vol. 9, no. 10, pp. 1620–1624, Oct. 2020.
- [19] X. Yuan, Q. Guo, X. Wang, and L. Ping, "Evolution analysis of low-cost iterative equalization in coded linear systems with cyclic prefixes," *IEEE J. Sel. Areas Commun.*, vol. 26, no. 2, pp. 301–310, Feb. 2008.
- [20] X. Yuan, C. Xu, L. Ping, and X. Lin, "Precoder design for multiuser MIMO ISI channels based on iterative LMMSE detection," *IEEE J. Sel. Top. Signal Process.*, vol. 3, no. 6, pp. 1118–1128, Dec. 2009.
- [21] X. Yuan, L. Ping, C. Xu, and A. Kavcic, "Achievable rates of MIMO systems with linear precoding and iterative LMMSE detection," *IEEE Trans. Inf. Theory*, vol. 60, no. 11, pp. 7073–7089, Nov. 2014.
- [22] L. Liu, Y. Chi, C. Yuen, Y. L. Guan, and Y. Li, "Capacity-achieving MIMO-NOMA: Iterative LMMSE detection," *IEEE Trans. Signal Process.*, vol. 67, no. 7, pp. 1758–1773, Apr. 2019.
- [23] S. Zhang and R. Zhang, "Capacity characterization for intelligent reflecting surface aided MIMO communication," *IEEE J. Sel. Areas Commun.*, vol. 38, no. 8, pp. 1823–1838, Aug. 2020.
- [24] V. Tervo, A. Tölli, J. Karjalainen, and T. Matsumoto, "Convergence constrained multiuser transmitter-receiver optimization in single-carrier fdma," *IEEE Trans. Signal Process.*, vol. 63, no. 6, pp. 1500–1511, 2015.
- [25] K. Shen and W. Yu, "Fractional programming for communication systems—part i: Power control and beamforming," *IEEE Trans. Signal Process.*, vol. 66, no. 10, pp. 2616–2630, May 2018.
- [26] S. Lin, B. Zheng, G. C. Alexandropoulos, M. Wen, F. Chen, and S. Mumtaz, "Adaptive transmission for reconfigurable intelligent surface-assisted OFDM wireless communications," *IEEE J. Sel. Areas Commun.*, vol. 38, no. 11, pp. 2653–2665, Nov. 2020.
- [27] Z. He and X. Yuan, "Cascaded channel estimation for large intelligent metasurface assisted massive MIMO," *IEEE Wireless Commun. Lett.*, vol. 9, no. 2, pp. 210–214, Feb. 2020.
- [28] H. Liu, X. Yuan, and Y.-J. A. Zhang, "Matrix-calibration-based cascaded channel estimation for reconfigurable intelligent surface assisted multiuser MIMO," *IEEE J. Sel. Areas Commun.*, vol. 38, no. 11, pp. 2621–2636, Nov. 2020.
- [29] M. Yue, L. Liu, and X. Yuan, "Practical RIS-aided coded systems: Joint precoding and passive beamforming," *IEEE Wireless Commun. Lett.*, vol. 10, no. 11, pp. 2345–2349, Nov. 2021.
- [30] J. Ma and H. Ge, "Groupwise successive interference cancellation for multirate cdma based on mmse criterion," in *Proc. IEEE Commun. Conf.*, vol. 2, 2000, pp. 1174–1178.
- [31] M. Varanasi, "Group detection for synchronous gaussian code-division multiple-access channels," *IEEE Trans. Inf. Theory*, vol. 41, no. 4, pp. 1083–1096, July 1995.
- [32] J. Luo, K. Pattipati, and P. Willett, "Optimal grouping and user ordering for sequential group detection in synchronous CDMA," in *Proc. IEEE GLOBECOM*, vol. 2, 2001, pp. 738–742.

- [33] M. Grant and S. Boyd, “CVX: Matlab software for disciplined convex programming, version 2.1,” <http://cvxr.com/cvx>, Mar. 2014.
- [34] S. Boyd, S. P. Boyd, and L. Vandenberghe, *Convex optimization*. Cambridge university press, 2004.
- [35] Y. Sun, P. Babu, and D. P. Palomar, “Majorization-minimization algorithms in signal processing, communications, and machine learning,” *IEEE Trans. Signal Process.*, vol. 65, no. 3, pp. 794–816, Feb. 2017.
- [36] D. Tse and P. Viswanath, *Fundamentals of wireless communication*. Cambridge university press, 2005.
- [37] N. Karmarkar, “A new polynomial-time algorithm for linear programming,” in *Proceedings of the sixteenth annual ACM symposium on Theory of computing*, 1984, pp. 302–311.
- [38] *NR; Multiplexing and channel coding*, Std. TR 38.212 version 17.0.0 Release 17, 3GPP, Jan. 2022.
- [39] M. Thomas and A. T. Joy, *Elements of information theory*. Wiley-Interscience, 2006.
- [40] H. Guo, Y.-C. Liang, J. Chen, and E. G. Larsson, “Weighted sum-rate maximization for reconfigurable intelligent surface aided wireless networks,” *IEEE Trans. Wireless Commun.*, vol. 19, no. 5, pp. 3064–3076, May 2020.